

Spherical fields as nonparaxial accelerating waves

Miguel A. Alonso^{1,*} and Miguel A. Bandres²

¹The Institute of Optics, University of Rochester, Rochester, New York 14627, USA

²Instituto Nacional de Astrofísica, Óptica y Electrónica Calle Luis Enrique Erro No. 1, Sta. Ma. Tonantzintla, Pue. CP 72840, Mexico

*Corresponding author: alonso@optics.rochester.edu

Received October 24, 2012; accepted November 9, 2012;

posted November 19, 2012 (Doc. ID 178481); published December 12, 2012

We introduce nonparaxial spatially accelerating waves whose two-dimensional transverse profiles propagate along semicircular trajectories while approximately preserving their shape. We derive these waves by considering imaginary displacements on spherical fields, leading to simple closed-form expressions. The structure of these waves also allows the closed-form description of pulses. © 2012 Optical Society of America

OCIS codes: 070.7345, 070.3185, 350.7420, 350.5500, 260.2110.

The so-called “accelerating waves” have received considerable attention due to their remarkable properties: they preserve their intensity profile under propagation, but the profile’s features follow a curved path. This behavior seems at odds with Ehrenfest’s theorem, which in this context states that the transverse intensity centroid of any free paraxial beam follows a straight path. The best-known example is that of Airy beams [1–3], although more general families of accelerating paraxial beams exist [4,5].

The strange behavior of these beams can be understood through two observations. First, their transverse intensity is not integrable, so they require infinite power and their transverse centroid is not well defined (i.e., Ehrenfest’s theorem is not violated). Second, they are associated with rays forming parabolic caustics, so the transverse intensity maximum is due to different ray bundles at different propagation distances. That is, one should not think of this maximum as a “physical entity” following a curved path. In real optical systems, the plane-wave spectrum is limited, leading to finite-power approximations to accelerating beams whose intensity profile is roughly preserved over some distance. While the intensity maximum of these beams still follows a curved path within this range, the now well-defined intensity centroid describes a straight line.

Nonparaxial accelerating waves in two dimensions, whose intensity profiles are roughly preserved within a range of propagation distances, and whose maxima follow semicircular paths, were recently proposed [6,7], based on the truncation of the backpropagating components of fields with cylindrical symmetry. Monochromatic and pulsed waves following other nonparaxial noncircular paths have also been implemented [8,9].

In this Letter, we extend these ideas to three-dimensional waves by starting with fields with rotational symmetry. Our solutions have a two-dimensional transverse intensity profile that is approximately invariant under propagation and whose maxima follow circular paths. To construct these waves we apply the concept of imaginary displacements [10]. By this means, unlike the solutions generated by imposing an abrupt exit pupil [6,7], we are able to give simple close-form expressions.

We begin by considering two-dimensional waves, i.e., solutions to the two-dimensional Helmholtz equation. One such solution is the Bessel field [11],

$$\psi_m(x, z) = u_0 i^m J_m \left[k \sqrt{x^2 + z^2} \right] \exp[im \arctan(z, x)], \quad (1)$$

where u_0 is a constant, m is an integer (assumed here to be positive), J_m is a Bessel function of the first kind, k is the wavenumber, (x, z) are Cartesian coordinates where z is regarded as the propagation direction, and $\arctan(\cos \phi, \sin \phi) = \phi$. This field has an intensity profile that is exactly preserved not over lines of constant z but over lines crossing the origin, and its maximum follows a circular caustic of radius m/k . Like in the paraxial regime, intensity maxima are slightly shifted away from the caustic. A section of this profile is shown in Fig. 1(a). For large m , the radial profile of this field approaches the profile of a paraxial Airy beam over a finite radial region near m/k . In fact, accurate approximations to these fields can be written in terms of Airy functions even for modest values of m [11].

Notice, though, that Bessel fields are composed of plane waves traveling in all directions:

$$\psi_m(x, z) = \int_{-\pi}^{\pi} A_m(\phi) \exp[ik(x \sin \phi + z \cos \phi)] d\phi, \quad (2)$$

where ϕ is the plane waves’ propagation angle from the z axis, and $A_m(\phi) = u_0 \exp(im\phi)/2\pi$ is the angular spectrum. Due to the finite NA of optical elements, it is difficult to generate in practice fields whose plane-wave

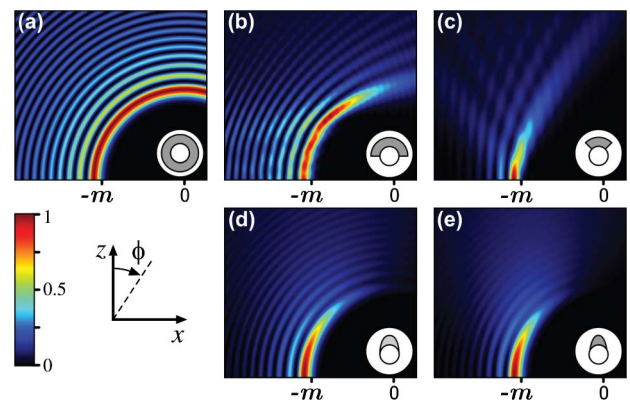


Fig. 1. (Color online) Intensities over a 90×80 rectangle (in units of k^{-1}) of $m = 40$ Bessel fields: (a) unapertured, apertured with (b) $\alpha = \pi$ and (c) $\alpha = \pi/2$, and apodized with (d) $q = 1.88$ and (e) $q = 3$. The insets indicate the power angular spectrum.

spectrum extends over all directions, so fields with spectra confined to forward propagation are usually considered. For this reason, Kammer *et al.* [6] proposed limiting the integration in Eq. (2) to $\phi \in [-\pi/2, \pi/2]$, which results in a forward-propagating wave with accelerating characteristics. Smaller ranges $\phi \in [-\alpha/2, \alpha/2]$ for $0 < \alpha \leq \pi$ can also be used. The intensities of these fields for $\alpha = \pi$ and $\pi/2$, are shown in Figs. 1(b) and 1(c), respectively. Notice that the intensity maximum propagates approximately along a circular path until its angle with respect to z is slightly below $\alpha/2$. However, for any $\alpha \neq 2\pi$, the fields must be evaluated numerically, and as shown in Figs. 1(b) and 1(c), the hard integration limits introduce appreciable rippling in the intensity.

To avoid these issues, we propose to use instead a Gaussian-like apodization factor $\exp[kq(\cos \phi - 1)]$ in the angular spectrum. This is formally equivalent to multiplying by $\exp(-q)$ and performing an imaginary shift $z \rightarrow z - iq/k$ [10]. The resulting field is given simply by

$$\psi_m(x, z; q) = \exp(-q)\psi_m(x, z - iq/k). \quad (3)$$

The intensities of these fields are shown in Figs. 1(d) and 1(e) for $q = 1.88$ and 3 . Note that the intensity maximum follows a circular path but decreases smoothly away from $z = 0$, and dissolves after tracing an angle of about $2 \arccos[I_1(q)/I_0(q)]$ with respect to z , with I_n being the modified Bessel function of the first kind. While these fields contain some counterpropagating components, these represent only a fraction $[1 - L_0(2q)/I_0(2q)]/2$ of the total power, where L_n is the modified Struve function of the first kind. For the cases in Figs. 1(d) and 1(e), this power fraction is about 1% and 0.082%, respectively.

We extend these ideas to create three-dimensional accelerating waves by using multipoles (separable in spherical coordinates), whose plane-wave spectra are spherical harmonics $Y_{l,m}$, aligned with the y axis for convenience:

$$\begin{aligned} \Lambda_l^m(\mathbf{r}) &= \int Y_l^m(\theta, \phi) \exp(ik\mathbf{r} \cdot \mathbf{u}) d\Omega \\ &= 4\pi i^l j_l \left(k \sqrt{x^2 + y^2 + z^2} \right) \\ &\quad \times Y_l^m \left[\arctan \left(y, \sqrt{x^2 + z^2} \right), \arctan(z, x) \right], \end{aligned} \quad (4)$$

where $\mathbf{r} = (x, y, z)$, j_l is a spherical Bessel function of the first kind, and the integral is over the unit vector $\mathbf{u} = (\sin \theta \sin \phi, \cos \theta, \sin \theta \cos \phi)$. These fields are associated with families of rays whose closest distance to the origin is $\sqrt{l(l+1)}/k \approx l/k$ and whose skew invariant around the y axis is m/k (both of which are related to the field's conserved total and azimuthal angular momentum, l and m), so the caustic is composed of segments of the sphere $r = l/k$ and the (two-sided) cone $\sin \theta = m/l$. We define spherical waves with imaginary displacements as

$$\Psi_n^m(\mathbf{r}; q) = u_0 \exp(-q) \Lambda_{m+n}^m(x, y, z - iq/k) \quad (5)$$

for $n \geq 0$. For $q = 0$ (no apodization) these fields have exact rotational symmetry about the y axis. For $q \gtrsim 2$, on

the other hand, the counterpropagating components are largely suppressed, and for $m \gg n$, these fields can be regarded as nonparaxial versions of Airy–Hermite–Gaussian beams, whose amplitude profile in y is a Hermite–Gauss function of order n (i.e., n specifies the number of zeroes in the y direction), while in the xz plane they behave as Airy beams. The intensity of some of these fields is shown in Figs. 2(a)–2(h). Of course, instead of apodizing through an imaginary displacement, one can define apertured versions where the integral in Eq. (4) is limited to a forward-propagating section of the sphere $[\sin \theta \cos \phi \geq \cos(\alpha/2)]$ and must be evaluated numerically. The case of half-spherical waves ($\alpha = \pi$) is shown in Figs. 2(i)–2(l). Whether apodized or apertured, these spherical waves present an intensity maximum (or maxima for $n > 0$) that follows a circular path of radius slightly larger than m/k , cf. Figs. 2(a), 2(e), and 2(i).

It is seen from Fig. 2 that, for larger n , the field's transverse intensity profile is noticeably curved, since one sheet of the caustic is spherical. The intensity then presents two cusps, one at each intersection of the spherical and conical caustic sheets [whose cross section is shown as a white line in Fig. 2(m)], and therefore resembles two joined Airy beams. One of the cusps can be suppressed, e.g., by combining three of these fields as

$$\Psi_n^m - \frac{i}{2}(\Psi_{n+1}^m - \Psi_{n-1}^m). \quad (6)$$

As shown in Fig. 2(n), this field's intensity at $z = 0$ resembles that of a single Airy beam whose cusp is approximately at $y = \sqrt{(2m+n)n}$, $x = -m/k$, but where one of the caustic sheets is curved. For $n \approx (\sqrt{2} - 1)m \gg 1$, this curvature becomes less appreciable and the field increasingly resembles an Airy beam.

The fields described so far are monochromatic. We now define closed-form pulsed solutions to the wave equation that follow similar paths. This is possible because in Eq. (4), k appears only as a factor in the argument of j_l , which can be written as a finite sum of powers times exponentials of its argument:

$$j_l(u) = \sum_{p=0}^l \frac{(2l-p)! [(-iu)^p \exp(iu) - (iu)^p \exp(-iu)]}{2^{l-p+1} i^l u^{l+1} p! (l-p)!}. \quad (7)$$

Substituting $u = \omega r/c$ (where ω is the frequency and c the speed of light) in Eq. (7) and multiplying by ω^{l+1} leads to an expression where each term includes ω as a non-negative power times an exponential. By using this result together with Eq. (4) and applying standard Fourier relations, we define the following pulsed solutions:

$$\begin{aligned} \mathcal{P}_n^m(\mathbf{r}, t) &= \int \tilde{f}(\omega) \omega^{m+n+1} \Lambda_{m+n}^m(\mathbf{r}) \exp(-i\omega t) d\omega \\ &= 4\pi Y_{m+n}^m(\theta, \phi) \left(\frac{ic}{2r} \right)^{m+n+1} \\ &\quad \times \sum_{p=0}^{m+n} \frac{(2m+2n-p)!}{p! (m+n-p)!} \left(\frac{2r}{c} \right)^p \\ &\quad \times \left[(-1)^p f^{(p)} \left(t + \frac{r}{c} \right) - f^{(p)} \left(t - \frac{r}{c} \right) \right], \end{aligned} \quad (8)$$

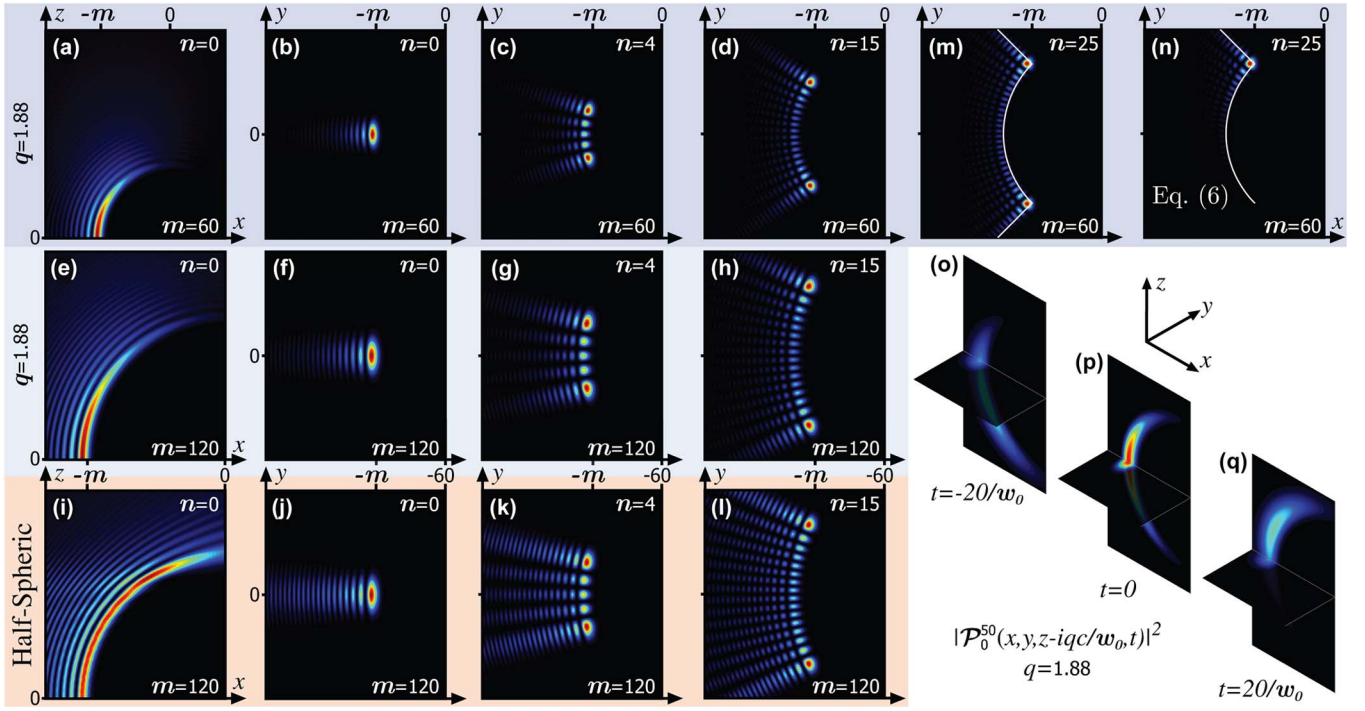


Fig. 2. (Color online) Intensities over sections of size 180×156 (in units of k^{-1}) of the $z = 0$ and $x = 0$ planes for (a)–(h), (m) the waves in Eq. (5) [(f) Media 1, (g) Media 2, (h) Media 3], (i)–(l) truncated spherical waves with $\alpha = \pi$, (n) the waves in Eq. (6), and (o)–(q) the pulses in Eq. (8) (Media 4). The caustic's cross section is shown in (m) and (n).

where $\tilde{f}(\omega)$ is an arbitrary spectrum, $f(t)$ is its inverse Fourier transform, $f^{(p)}$ is the p th derivative of f , and (r, θ, ϕ) are spherical coordinates with respect to the y axis. Figures 2(o)–2(q) show cross sections at three times for such a pulse for $f(t) = \exp(-t^2 \Delta^2/2 - i\omega_0 t)$ [for which $f^{(p)}$ can be expressed in terms of Hermite polynomials] with $\Delta = \omega_0/10$, $m = 50$, $n = 0$, and using an imaginary displacement in z of size $1.88c/\omega_0$. As in the monochromatic case, for larger n these pulses display two cusps, one of which can be eliminated through the combination $\mathcal{P}_n^m - (\mathcal{P}_{n+1}^m + \mathcal{P}_{n-1}^m)/2$. Note that, unlike the pulses in [9], these pulses do not run along the caustic, but rather inhabit it simultaneously at a given range of times.

In conclusion, we proposed nonparaxial accelerating fields given by simple closed-form expressions. While these fields are scalar, polarization can be easily incorporated by either using vector multipoles or applying suitable operators. Also, the paths followed by the maxima are circular due to the use of solutions separable in spherical coordinates. Using other coordinate systems would result in other shapes of the caustic sheets.

M. A. Alonso acknowledges support from the National Science Foundation (PHY-1068325).

References

1. M. V. Berry and N. L. Balazs, *Am. J. Phys.* **47**, 264 (1979).
2. G. A. Siviloglou, J. Broky, A. Dogariu, and D. N. Christodoulides, *Phys. Rev. Lett.* **99**, 213901 (2007).
3. S. Vo, K. Fuerschbach, K. P. Thompson, M. A. Alonso, and J. P. Rolland, *J. Opt. Soc. Am. A* **27**, 2574 (2010).
4. M. A. Bandres, *Opt. Lett.* **33**, 1678 (2008).
5. M. A. Bandres, *Opt. Lett.* **34**, 3791 (2009).
6. I. Kaminer, R. Bekenstein, J. Nemirovsky, and M. Segev, *Phys. Rev. Lett.* **108**, 163901 (2012).
7. P. Zhang, Y. Hu, D. Cannan, A. Salandrino, T. Li, R. Morandotti, X. Zhang, and Z. Chen, *Opt. Lett.* **37**, 2820 (2012).
8. L. Froehly, F. Courvoisier, A. Mathis, M. Jacquot, L. Furfaro, R. Giust, P. A. Lacourt, and J. M. Dudley, *Opt. Express* **19**, 16455 (2011).
9. F. Courvoisier, A. Mathis, L. Froehly, R. Giust, L. Furfaro, P. A. Lacourt, M. Jacquot, and J. M. Dudley, *Opt. Lett.* **37**, 1736 (2012).
10. M. V. Berry, *J. Phys. A* **27**, L391 (1994).
11. M. V. Berry, *Sci. Prog.* **57**, 43 (1969).